Journal of Reproduction and Development, Vol. 70, No 6, 2024

Original Article

Change in the ability of bovine granulosa cells to elongate transzonal projections and their transcriptome changes during follicle development

Mihoko FUSHII[1)], Hirohisa KYOGOKU[1)], Jibak LEE[1)] and Takashi MIYANO[1)]

[1)]*Laboratory of Developmental Biotechnology, Graduate School of Agricultural Science, Kobe University, Kobe 657-8501, Japan*

Abstract. Granulosa cells (GCs) in secondary follicles differentiate into cumulus cells (CCs) and mural granulosa cells (MGCs) in the antral follicle. Only CCs maintain direct connections with oocytes through transzonal projections (TZPs) and support oocyte growth. Here, we examined whether granulosa cells (GCs) from secondary follicles and MGCs from early and late antral follicles were able to reconstruct complexes with TZP-free denuded oocytes (DOs) and regenerate TZPs. Furthermore, to confirm that the regenerated TZPs were functional, the development of the reconstructed complexes and oocyte growth in the complexes were evaluated. After coculture, GCs and MGCs from early antral follicles reconstructed the complexes with DOs and regenerated TZPs. Furthermore, the oocytes in the integrally reconstructed complexes grew fully and acquired meiotic competence, suggesting that the regenerated TZPs were functional. In contrast, MGCs from the late antral follicles lost their ability to elongate TZPs. As the ability to regenerate TZPs differed among cells, we analyzed the transcriptomes of GCs, CCs, and MGCs collected from follicles of different sizes. The characteristics of TZP generation coincided with the transcriptome changes in two directions: from GCs to CCs and MGCs. In conclusion, until the early antral follicle stage, bovine GCs, CCs, and MGCs have common characteristics to elongate TZPs and form antrum-like structures that support oocyte growth *in vitro*. Furthermore, as the follicle develops, MGCs lose the ability to elongate TZPs.

Key words: Bovine granulosa cell, Cumulus cell, Mural granulosa cell, Transzonal projection, Oocyte growth

(**J. Reprod. Dev. 70:** 362–371, 2024)

During secondary follicle to early antral follicle development, granulosa cells (GCs) differentiate into cumulus cells (CCs), which surround the oocyte, and mural granulosa cells (MGCs), which line the follicle wall [1, 2]. These two cell types have different phenotypes and roles in the follicle [2, 3]. MGCs play a role in estrogen synthesis and control the estrous cycle. In contrast, CCs maintain direct connections with oocytes through transzonal projections (TZPs) and support oocyte growth. Although MGCs do not contact oocytes, they indirectly support oocyte growth in a paracrine manner [4–6]. MGCs produce natriuretic peptide precursor C (NPPC), which stimulates natriuretic peptide receptor 2 (NPR2) in CCs and increases cyclic guanosine monophosphate (cGMP) levels. cGMP is transported to oocytes via TZPs and maintains oocyte meiotic arrest [6, 7]. As the antrum develops, growing oocytes acquire the ability to resume meiosis [8–10]. CCs and MGCs cooperatively prevent precocious meiotic resumption of growing oocytes [11–14]. Although MGCs and CCs play different roles, they cooperate during the growth and meiotic arrest of oocytes in the antral follicles.

The default pathway of GC differentiation proceeds to the MGC phenotype [15] and oocyte-derived factors such as growth differentiation factor 9 (GDF9) and bone morphogenetic protein 15 (BMP15) promote GC differentiation into the CC phenotype [3, 16]. In mice, some studies showed that MGCs and CCs express different subsets of transcripts in the antral follicles [17, 18] and that oocytes control the expressions of multiple genes in CCs [19, 20]. These studies support the hypothesis that a concentration gradient of oocyte-derived factors in the antral follicles is responsible for the different roles of these two cell types.

We previously showed that MGCs from bovine early antral follicles adhered to TZP-free denuded oocytes (DOs) and directly supported oocyte growth through TZPs like CCs [21]. However, it remains unknown whether MGCs maintain the ability to elongate TZPs during antral follicle development and whether this ability is related to the transcriptome of each follicular cell type.

This study was conducted to clarify whether bovine GCs, after differentiating into MGCs and during further antral follicle development, maintain the ability to support oocyte growth *via* TZPs and to examine the relationship between this ability and the transcriptome of the cell type. Using oocyte and MGC reconstitution methods [21] (Supplementary Fig. 1), we examined whether GCs from secondary follicles and MGCs from late antral follicles were able to reconstruct complexes with TZP-free DOs and regenerate TZPs similar to MGCs from early antral follicles. To confirm whether the regenerated TZPs were functional, the integrity of the reconstructed complexes and antrum formation were examined throughout the subsequent growth culture period. After culture, the TZP count, oocyte diameter, and meiotic competence were determined. The transcriptomes of GCs, CCs, and MGCs from the three differently sized follicles were analyzed.

Materials and Methods

Chemicals

All chemicals were purchased from Sigma-Aldrich (St. Louis, MO, USA) unless otherwise stated.

Received: February 23, 2024
Accepted: August 14, 2024
Advanced Epub: October 14, 2024

Correspondence: M Fushii (e-mail: mihoko.fushii@riken.jp)

Collection of DOs, GCs, and MGCs

Oocyte-cumulus cell-mural granulosa cell complexes (OCGCs) were collected from early antral follicles (0.5–0.7 mm in diameter) as described previously [22, 23]. Denuded oocytes (DOs) and mural granulosa cells (MGCs) were collected from OCGCs as described previously [21] (Supplementary Fig. 1). Bovine ovaries were obtained from a local slaughterhouse and transported to the laboratory. The ovaries were washed once with 0.2% (w/v) cetyltrimethylammonium bromide (FUJIFILM Wako Pure Chemical Corporation, Osaka, Japan) and three times with Dulbecco's phosphate-buffered saline (PBS) containing 0.1% (w/v) polyvinyl alcohol (PVA) (PBS-PVA). Ovarian cortical slices were collected using surgical blades (No. 21; ELP, Akiyama-seisakusyo, Tokyo, Japan) and forceps. Early antral follicles (0.5–0.7 mm in diameter) were dissected from ovarian cortical slices in 25 mM HEPES (Dojindo Laboratories, Kumamoto, Japan) -buffered medium 199 (Nissui Pharmaceutical, Tokyo, Japan) (HEPES-199) containing 0.1% (w/v) PVA, 0.85 mg/ml sodium bicarbonate (FUJIFILM Wako Pure Chemical Corporation), and 0.08 mg/ml kanamycin sulfate. The follicles were opened using a surgical blade (No. 10; Feather Safety Razor, Tokyo, Japan) and forceps to collect the OCGCs containing growing oocytes. MGCs were also collected from late antral follicles (4–6 mm in diameter).

Oocyte-granulosa cell complexes (OGCs) were collected from bovine secondary follicles (0.2–0.4 mm in diameter) to prepare granulosa cells (GCs). Oocytes were removed from the OGCs using a narrow pipette, and the GCs were collected.

The diameter of oocytes in OCGCs and DOs (excluding the zona pellucida) from early antral follicles was measured to the nearest 1 µm under an ocular micrometer (Olympus Corporation, Tokyo, Japan) attached to an inverted microscope. Oocytes with diameters 90–105 µm were selected for further analysis.

OCGCs containing fully grown oocytes with diameters of at least 115 µm were collected from late antral follicles and aspirated with follicular fluid using a syringe and needle (18 GA; Terumo Corporation, Tokyo, Japan). Cumulus cells (CCs) and MGCs were removed completely from the OCGCs using a narrow pipette, and the diameters of the collected DOs were measured. Oocytes with diameters of 115 µm or more served as the *in vivo* fully grown control [9].

Reconstruction of DO+GC/MGC complexes

To prepare TZP-free DOs, groups of 4–14 DOs collected from early antral follicles from at least three biological replicates were cultured individually in 12 µl microdrops of culture medium covered with paraffin oil in Petri dishes (Falcon No. 351007; BD Biosciences, Franklin Lakes, NJ, USA) at 38.5°C under a controlled humidified atmosphere of 5% O_2, 5% CO_2, and 90% N_2 for 24 h as described previously [21]. The basic culture medium was α-minimum essential medium (αMEM, Cat. No. 11900-024; Invitrogen, Carlsbad, CA, USA) supplemented with 5% (v/v) fetal bovine serum (FBS; ICN Biomedicals, Aurora, OH, USA), 50 µg/ml ascorbic acid 2-glucoside (Hayashibara Biochemical Laboratories, Okayama, Japan), 55 µg/ml cysteine, 0.05 µM dexamethasone, 4 mM hypoxanthine, 4% (w/v) polyvinylpyrrolidone (molecular weight 360,000), 2.2 mg/ml sodium bicarbonate, and 0.08 mg/ml kanamycin sulfate [24]. Based on a previous report [23], the culture medium was supplemented with 10 ng/ml 17β-estradiol and 10 ng/ml androstenedione (Tokyo Chemical Industry, Tokyo, Japan).

To reconstruct oocyte-granulosa cell complexes and oocyte-mural granulosa cell complexes, 2–3 masses of GCs from secondary follicles and masses of MGCs, larger than those of DOs, from early and late antral follicles were prepared as described above. Collected GCs and MGCs were cocultured with TZP-free DOs individually in 12 µl microdrops of the culture medium in Petri dishes (Falcon No. 351007) for 24 h. After coculture, the reconstructed complexes in which GCs and MGCs adhered to DOs (DO+GCs and DO+MGCs) were transferred to Millicell inserts (cell culture inserts 0.4 µm, 30 mm diameter; Merck Millipore, Darmstadt, Germany) in Petri dishes (Falcon No. 351008) and cultured for 4 or 12 days. The reconstructed complexes were cultured at 38.5°C under a controlled humidified atmosphere of 5% O_2, 5% CO_2, and 90% N_2 for 5 days, followed by culture in an atmosphere of 5% CO_2 in the air for 7 days [25]. The day on which the DOs were collected was designated as day 0, and half of the culture medium was replaced with fresh medium every other day after day 6.

Fluorescence microscopy

To identify transzonal projections (TZPs) rich in actin filaments, fluorescence microscopy was performed as previously described [21, 23]. Briefly, oocytes surrounded by CCs or MGCs were mechanically denuded. The DOs were washed twice with PBS-PVA and fixed in 4% paraformaldehyde in PBS-PVA for 60 min. After washing twice with PBS-PVA, fixed oocytes were stored in PBS-PVA containing 1 mg/ml bovine serum albumin (BSA) (PBS-PVA-BSA) at 4°C overnight. The oocytes were then incubated with Alexa Fluor 488 conjugated phalloidin (8.25 nM in PBS-PVA-BSA; Cat. No. A12379; Molecular Probes, Eugene, OR, USA) at 38.5°C under a controlled atmosphere (5% CO_2 in air) for 90 min. The cells were washed three times for 15 min each in PBS-PVA-BSA and mounted on glass slides with ProLong Gold antifade reagent with DAPI (Cat. No. P36931; Molecular Probes). The TZPs were visualized using a confocal laser scanning microscope (FV1000-KDM; Olympus Corporation). The number of visible actin-based TZPs that penetrated the zona pellucida and reached the oocyte surface was counted in the widest oocyte section.

In vitro growth culture of complexes

In vitro growth culture of DO+GCs and DO+MGCs (24 h after denudation and 24 h of reconstruction) was performed on Millicell inserts, as described above, for 12 days (total of 14 days). As the control, groups of 9–14 OCGCs collected from early antral follicles from at least 7 biological replicates were cultured for 14 days on Millicell inserts placed in Petri dishes (Falcon No. 351008) under the same conditions at 38.5°C with a controlled humidified atmosphere of 5% O_2, 5% CO_2, and 90% N_2 for 7 days, followed by an atmosphere of 5% CO_2 in air for 7 days [25]. Formation of antrum-like structures by the complexes was examined daily by identifying the visible spaces surrounded by somatic cells. Complexes with cytoplasmic degenerative oocytes, detachment of somatic cells from the zona pellucida, and collapsed complexes were classified as disintegrated complexes, whereas all others were regarded as complexes that maintained their integrity.

After culture, the diameters of the oocytes were measured as described above. Some oocytes were mechanically denuded to examine the number of TZPs or stages of meiosis. The number of TZPs was determined as described above. To assess the meiotic stage, the oocytes were fixed in acetic acid-ethanol (1:3) and stained with 1% (w/v) aceto-orcein (FUJIFILM Wako Pure Chemical Corporation). The stages of meiotic division were assessed using Nomarski interference microscopy. Oocytes are classified based on the morphology of the chromatin and nuclear envelope [21, 26, 27]. The oocyte stages before meiotic resumption were classified as filamentous chromatin

(FC), stringy chromatin (SC), and germinal vesicle I–IV (GV I–IV). After the resumption of meiosis, the stages were classified as early diakinesis (ED), late diakinesis (LD), metaphase I (MI), anaphase I and telophase I (AI-TI), and metaphase II (MII). Oocytes with cytoplasmic or nuclear abnormalities were considered degenerate. The meiotic stages of oocytes collected from the late antral follicles were also examined and served as *in vivo* controls.

In vitro maturation culture of complexes

DO+GCs, DO+MGCs, and OCGCs that maintained their integrity after *in vitro* growth culture were used to analyze *in vitro* maturation, as described previously [21, 22]. OCGCs collected from early and late antral follicles were matured and served as *in vivo* controls. Briefly, complexes were cultured in 50 µl microdrops of maturation medium covered with paraffin oil at 38.5°C under a controlled atmosphere (5% CO_2 in air) for 22 h. Each microdrop contained three to five complexes collected from at least four biological replicates. The maturation medium was TCM-199 (Nissui Pharmaceutical) supplemented with 10% (v/v) FBS, 0.1 mg/ml sodium pyruvate (Nacalai Tesque, Kyoto, Japan), 2.2 mg/ml sodium bicarbonate, 0.08 mg/ml kanamycin sulfate, and 0.1 IU/ml human menopausal gonadotropin (Aska Pharmaceutical, Tokyo, Japan).

After 22 h, the oocytes were mechanically denuded using 0.1% (w/v) hyaluronidase and a narrow pipette. The oocytes were fixed with acetic acid-ethanol (1:3) and stained with 1% (w/v) aceto-orcein to assess the stage of oocyte maturation.

RNA sequencing analysis

RNA sequencing libraries were constructed to perform RNA sequencing (RNA-seq) analysis of GCs collected from secondary follicles and CCs and MGCs collected from early and late antral follicles. To prepare CCs, oocyte-cumulus cell complexes (OCCs) were collected from early and late antral follicles as described previously [22]. Briefly, as many MGCs as possible were removed from the OCGCs using a narrow pipette. The resulting complexes composed of growing oocytes surrounded by two or three layers of CCs were referred to as OCCs. Oocytes were removed from the OCCs using a narrow pipette, and the CCs were collected.

Total RNA extraction, first-strand cDNA synthesis, cDNA amplification, and sequencing library generation were performed with 1/2 volumes of the SMART-Seq v4 Ultra Low Input RNA Kit (Takara Bio, Shiga, Japan) and a Nextera XT DNA Library Preparation Kit (Illumina, San Diego, CA, USA) according to the manufacturer's protocols. Twelve PCR cycles were applied to the DNA library. After PCR, the DNA library was purified using SPRIselect (Beckman Coulter, Brea, CA, USA) rather than using AMPure XP beads (Beckman Coulter). Library sequencing was performed on a HiSeq X (Illumina). Four GCs collected from secondary follicles and five CCs and five MGCs collected from early and late antral follicles were sequenced.

Sequence data analysis

RNA-seq reads were processed before analysis as described previously [28] with some modifications. Hisat2 (v2.1.0) [29] with '-p 16 -x' options was used to map the reads to the ARS-UCD1.2.105 genome assembly of the bovine genome after trimming adaptor sequences and low-quality bases using fastp (v0.20.0) [30] with '-w 16 --trim-poly-x --detect_adapter_for_pe_h' options. The resulting binary alignment/map (BAM) files were sorted using Samtools (v1.10) [31]. The featureCounts (v2.0.0) [32] tool of Subread package with '-T 16 -F GTF -t exon -g gene_id -p -o' options was used to generate counts of reads multi-mapped to annotated genes using the gene annotation for *Bos taurus* (Ensembl, ARS-UCD1.2.105).

Based on the $\log_{10}$ transformed transcripts per kilobase million (TPM) values of expression, principal component analysis (PCA) was conducted using R (https://www.r-project.org/), *t*-distributed stochastic neighbor embedding (*t*-SNE) plots were visualized using Rtsne package (v0.16) [33], and marker genes for clusters were searched using MGFR package (v1.22.0) [34] in R.

Differentially expressed genes (DEGs) (false discovery rate, FDR < 0.05) were identified using edgeR package (v3.38.1) [35] in R, which normalizes library sizes with the trimmed mean of M values (TMM) method, using the dataset of genes expressed in at least one sample. Gene Ontology (GO) analysis was performed using g:Profiler (e109_eg56_p17_773ec798) (https://biit.cs.ut.ee/gprofiler/gost) [36].

Data availability

RNA-seq data for bovine GCs, CCs, and MGCs were deposited in the Gene Expression Omnibus (GEO) repository and are accessible under accession number GSE255879.

Statistical analysis

The differences between the mean (± SEM) diameters of *in vitro*- and *in vivo*-grown oocytes and mean number of TZPs were analyzed using one-way ANOVA followed by Tukey-Kramer multiple range test (Excel software with the add-in Ekuseru-Toukei 2010). The number of TZPs was also analyzed using Smirnov-Grubbs' outlier test ($P < 0.05$). All other experimental data, except the RNA-seq data, were analyzed using chi-square test. Statistical significance was set at $P < 0.05$.

Results

Reconstruction of DO+GC/MGC complexes and regeneration of TZPs

TZP-free DOs were cultured with GCs and MGCs from two different follicle stages for six days to examine the reconstruction of complexes. The typical morphologies of DO+GCs and DO+MGCs during growth culture are shown in Fig. 1A. Oocytes collected from early antral follicles were denuded (Fig. 1A, a0, b0, c0). At 24 h after denudation, the DOs were cocultured with two to three masses of GCs from secondary follicles (referred to as "GCs") (Fig. 1A, a1), and masses of MGCs from early and late antral follicles (referred to as "early MGCs" and "late MGCs," respectively) (Fig. 1A, b1, c1). After coculture for 24 h, GCs and early MGCs adhered to the DOs and culture substrate (Fig. 1A, a2, b2). All DOs maintained on the masses of GCs and early MGCs for 24 h after the start of coculture were surrounded by GCs and MGCs, and complexes (DO+GCs and DO+early MGCs) were reconstructed. After subsequent culture on the inserts, the reconstructed complexes were attached to membrane sheets and developed as spherical structures (Fig. 1A, a3, b3). In contrast, after coculture for 24 h, most of the late MGCs barely adhered to the DOs and culture substrate (Fig. 1A, c2). After transfer onto Millicell inserts, these complexes did not attach to the membrane sheets. Late MGCs aggregated tightly and oocytes were pushed out of the complexes during culture (Fig. 1A, c3). On day 6, although 39% of late MGCs contained oocytes, it was difficult to mechanically denude the oocytes from these complexes, and the oocytes in these complexes degenerated. The remaining almost denuded oocytes (61%) were used to examine the regeneration of TZPs.

On day 6, regenerated TZPs were observed in oocytes cocultured with GCs and early MGCs (Fig. 2A, a1, b1), and the number of TZPs

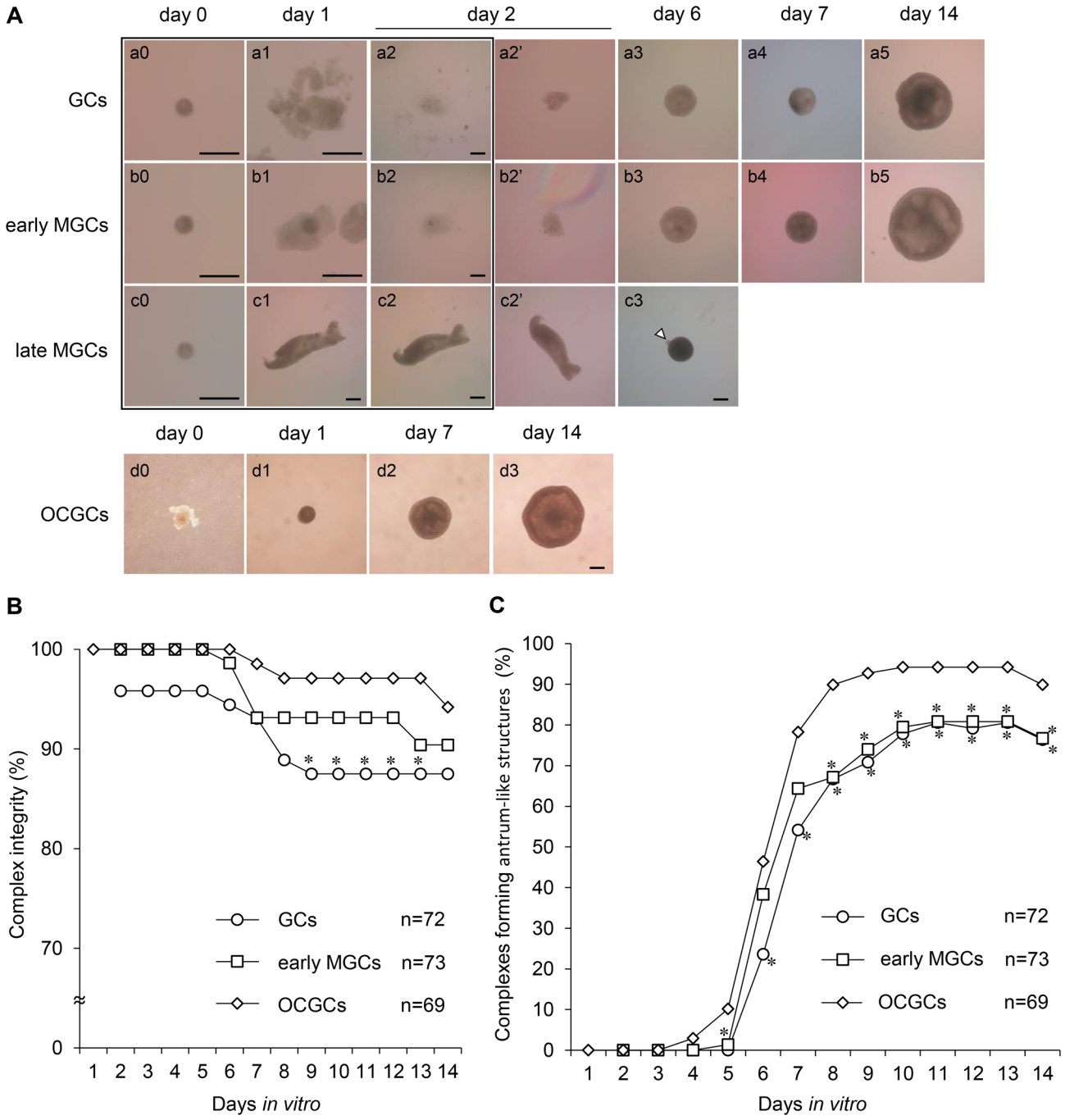

Fig. 1. Typical morphologies of bovine DO+GC/MGC complexes and OCGCs during *in vitro* growth culture (A), integrity of reconstructed complexes and OCGCs (B), and formation of antrum-like structures (C). (A) DOs collected from early antral follicles (0.5–0.7 mm) cultured in microdrops of culture medium (a0, b0, c0). DOs were cocultured with GCs (a1), early MGCs (b1), or late MGCs (c1) 24 h after denudation (day 1). After coculture for 24 h (day 2), DO+GCs (a2) and DO+MGCs (b2, c2) were transferred to Millicell inserts (a2', b2', c2') and further cultured (a3–5, b3–5, c3). On day 6, late MGCs aggregated tightly, and some oocytes were pushed out of the complexes during culture (c3). Arrowhead indicates a pushed-out oocyte. Images framed in black indicate DOs, DO+GCs, and DO+MGCs cultured in the microdrops. As a control, OCGCs collected from early antral follicles were cultured on Millicell inserts for 14 days (d0–3). Scale bars represent 200 µm. (B and C) Complex integrity and antrum-like structure formation by GCs and early MGCs cocultured with DOs. DO+GCs and DO+early MGCs were examined after the start of coculture. Number of complexes (n) used in each group is shown in each graph. * Values are significantly different from those of OCGCs ($P < 0.05$).

was increased compared to that in oocytes at 24 h after denudation (Fig. 2B). However, regenerated TZPs were not observed in 93% of oocytes cocultured with late MGCs (Fig. 2A, c1; Fig. 2B). Therefore, this experimental group was excluded from further analyses.

Development of reconstructed complexes and oocyte growth

During growth culture for up to 14 days, the reconstructed complexes with GCs (Fig. 1A, a4, 5) and early MGCs (Fig. 1A, b4, 5) grew similarly to control OCGCs (Fig. 1A, d2, 3). The integrity of the reconstructed complexes and OCGCs during culturing is shown in Figure 1B. On day 2, 96% of the DOs were surrounded by GCs,

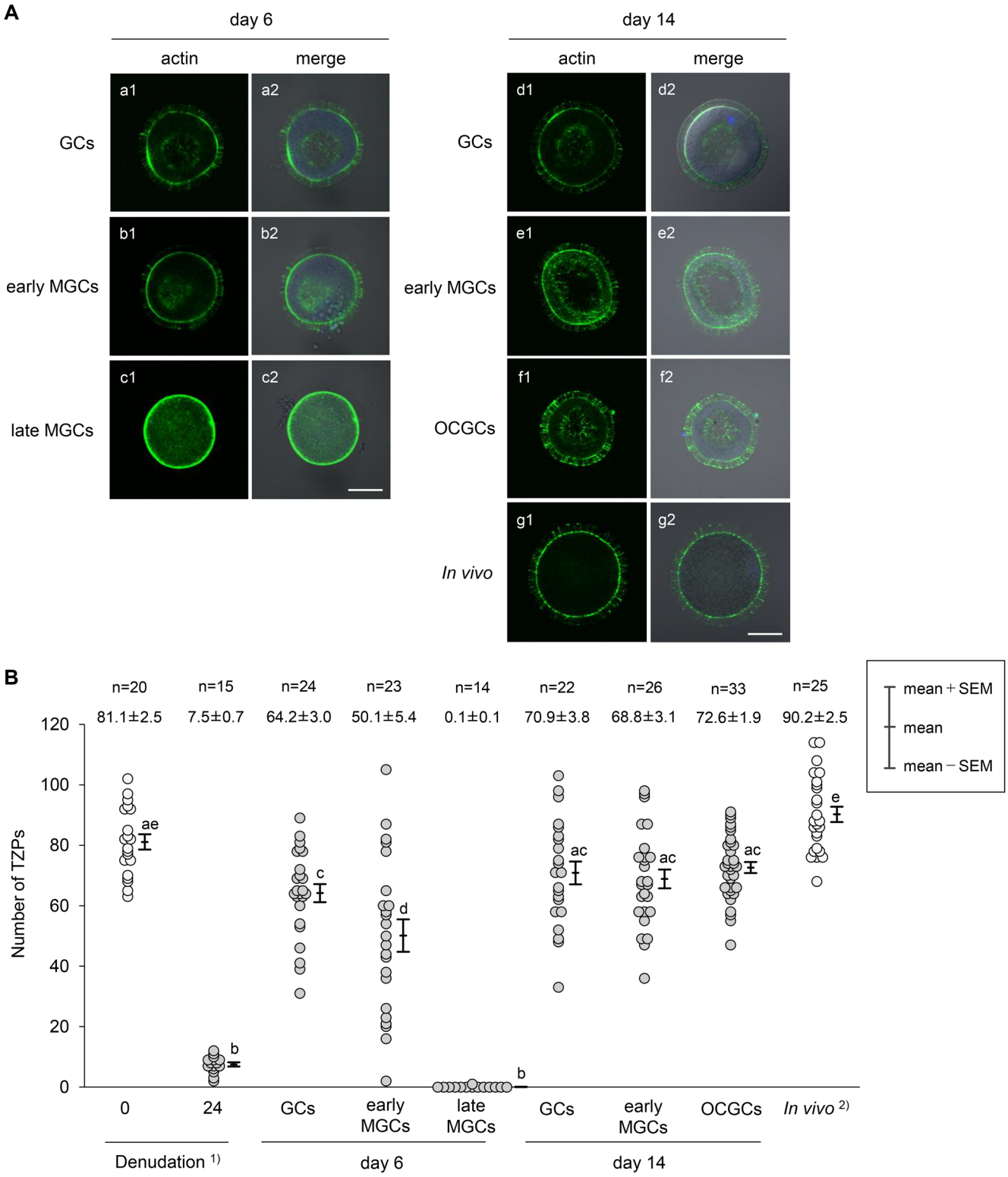

Fig. 2. Fluorescence staining of bovine oocytes showing TZPs in reconstructed complexes (A) and changes in the number of TZPs in bovine oocytes in reconstructed complexes (B) during *in vitro* growth culture. (A) On day 6, regenerated TZPs were observed in oocytes cocultured with GCs (a1) and early MGCs (b1). However, few regenerated TZPs were observed in oocytes cocultured with late MGCs (c1). On day 14, many TZPs in reconstructed complexes (d1, e1) penetrated the zona pellucida to reach the oocyte surface in a manner similar to TZPs in OCGCs (f1) and *in vivo*-fully grown oocytes (g1). Alexa Fluor 488 conjugated phalloidin stained F-actin green (a1–g1), and DAPI stained chromatin blue. Bright-field images are merged with fluorescent staining images (a2–g2). Nucleus was often not observed in the widest cross-section of the oocyte because the images were out of focus. Scale bars represent 50 µm. (B) Number of visible actin-based TZPs that penetrated the zona pellucida to reach the oocyte surface was counted in the widest cross-section of the oocytes. Number of oocytes (n) used in each group and the mean (± SEM) number of TZPs are shown at the top. [1)] DOs collected from early antral follicles and cultured for 24 h. [2)] *In vivo*-fully grown oocytes collected from late antral follicles. [a–e] Different letters denote significantly different values ($P < 0.05$).

and all DOs were surrounded by early MGCs. As some of the DOs were distant from and not surrounded by GCs and early MGCs during coculture, the integrity of the reconstructed complexes was decreased. On day 7, 93% of reconstructed complexes and 99% of OCGCs maintained their structures. However, as the coculture progressed, some structures of the reconstructed complexes and OCGCs collapsed, and the oocytes became denuded. On day 14, OCGCs showed higher integrity than DO+GCs and DO+early MGCs (94%, 88%, and 90%, respectively).

As the complexes developed, more than 75% of complexes formed antrum-like structures (Fig. 1A, a3–5, b3–5, d2, 3). OCGCs started to form antrum-like structures on day 4, which was one to two days earlier than observed for the reconstructed complexes (Fig. 1C). On day 14, OCGCs showed higher rates of antrum-like structure formation than DO+GCs and DO+early MGCs (90%, 76%, and 77%, respectively).

After 14 days of growth culture, many TZPs in the reconstructed complexes penetrated the zona pellucida to reach the oocyte surface in a manner similar to that of TZPs in OCGCs and *in vivo* fully grown oocytes (Fig. 2A, d1–g1). The mean numbers of TZPs in DO+GCs and DO+early MGCs (70.9 ± 3.8 and 68.8 ± 3.1, respectively) were similar to those in OCGCs (72.6 ± 1.9) and *in vivo*-growing oocytes (81.1 ± 2.5, Denudation 0 in Fig. 2B), although the value was smaller than that in *in vivo* fully grown oocytes (90.2 ± 2.5) (Fig. 2B).

The mean diameters of oocytes grown in reconstructed complexes with GCs and early MGCs, and in OCGCs increased significantly (116.0 ± 1.1, 117.8 ± 0.9, and 119.0 ± 0.8 µm, respectively) compared to that of oocytes before culture, although they were smaller than *in vivo* fully grown oocytes (126.5 ± 0.5 µm) (Fig. 3).

Growing oocytes collected from early antral follicles were at the FC or SC stage, whereas all *in vivo* fully grown oocytes collected from late antral follicles were at the GV stage (Table 1A). After growth culture, 50% of oocytes in DO+GCs, 74% of oocytes in DO+early MGCs, and 69% of oocytes in OCGCs reached the GV stage. In subsequent maturation culture, 61%, 75%, and 71% of oocytes in DO+GCs, DO+early MGCs, and OCGCs, respectively, reached MII (Table 1B). Most growing oocytes collected from the early antral follicles remained at the FC stage after maturation culture, whereas all fully-grown oocytes collected from the late antral follicles reached MII.

Transcriptome analysis of CCs, GCs, and MGCs

Because culture experiments with DO+GC/MGC complexes suggested that late MGCs lost the ability to elongate TZPs, transcriptome changes were analyzed among GCs, early MGCs, and late MGCs. CCs from early and late antral follicles (referred to as "early CCs" and "late CCs") were also analyzed.

First, datasets from GCs, early CCs, late CCs, early MGCs, and late MGCs were analyzed using PCA and *t*-SNE dimensionality analyses, and the expression of marker genes was visualized (Fig. 4). PCA revealed changes from GCs to early and late MGCs along the PC2 axis, and changes from GCs to late CCs along the PC1 axis (Fig. 4A). *t*-SNE analysis showed that each cell type formed a cluster (Fig. 4B). Early CCs, early MGCs, late CCs, and late MGCs formed well-separated clusters, whereas GCs did not form a discrete cluster. Instead, GCs partially overlapped with early CCs and early MGCs clusters. The heatmap shows a distinct gene expression pattern in each cell group (Fig. 4C), and marker genes for each cell group were identified (Fig. 4C, right column, and Supplementary Table 1).

GO analysis of the DEGs revealed distinct characteristics in the transcriptomes between the group of GCs, early CCs, and early MGCs (referred to as the "early group") and the late MGCs group or late CCs group. Comparison of the datasets from the early group to those of the late MGCs group revealed a substantial number of DEGs (up-regulated genes: n = 1,943; down-regulated genes: n = 1,716) (Supplementary Table 2). Figure 5A shows that genes involved in the "developmental process" were mainly up-regulated in the early group. In contrast, genes involved in "organonitrogen compound metabolic process," "ribosome biogenesis," and "protein folding" were mainly down-regulated in the early group (Fig. 5B).

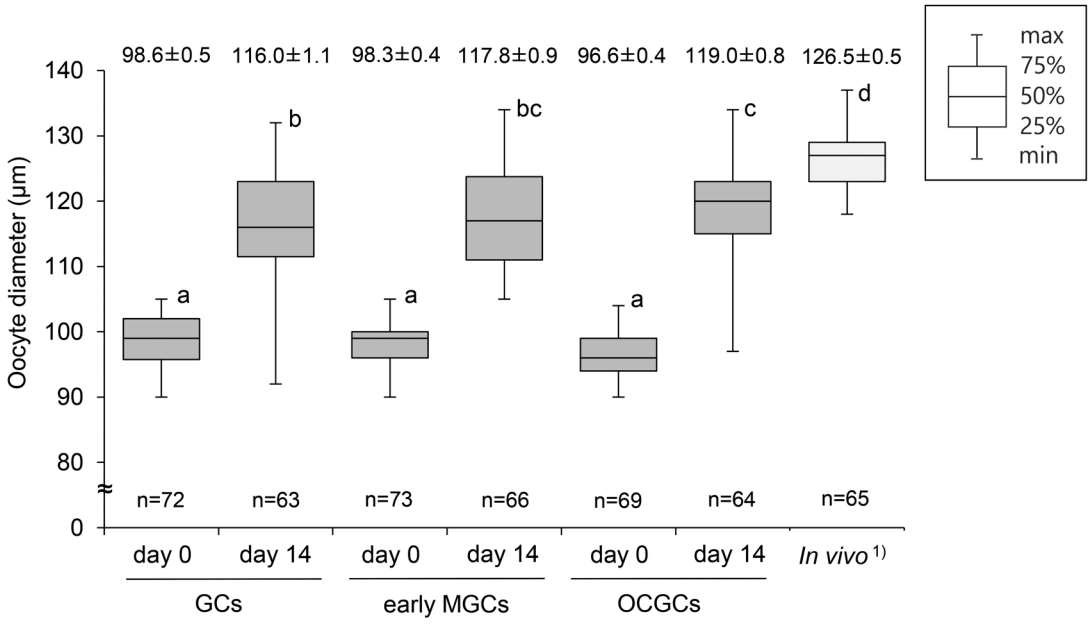

Fig. 3. Diameters of bovine oocytes in reconstructed complexes after *in vitro* growth culture. DOs were cocultured with GCs and early MGCs. Number of oocytes (n) used in each group is shown at the bottom of each box. Mean (± SEM) diameters of oocytes are shown at the top of each box. [1)] Diameter of fully grown oocytes collected from late antral follicles (4–6 mm). [a–d] Different letters denote significantly different values ($P < 0.05$).

Table 1. Meiotic stages (A) and competence (B) of *in vitro*-grown bovine oocytes in reconstructed complexes

(A)

In vitro growth (day)	Types of complexes [1]	Number of oocytes used	Number (%) of oocytes at each stage [5]								
			FC	SC	GV	ED	LD	MI	AI-TI	MII	DG
0 [3]	-	24	11 (46)	13 (54)	0 (0)	0 (0)	0 (0)	0 (0)	0 (0)	0 (0)	0 (0)
14	GCs	18	3 (17)	2 (11)	9 (50)	0 (0)	0 (0)	1 (6)	0 (0)	0 (0)	3 (17)
	early MGCs	19	0 (0)	1 (5)	14 (74)	0 (0)	1 (5)	0 (0)	0 (0)	0 (0)	3 (16)
	OCGCs	16	1 (6)	0 (0)	11 (69)	2 (13)	0 (0)	0 (0)	0 (0)	0 (0)	2 (13)
In vivo [4]	-	20	0 (0)	0 (0)	20 (100)	0 (0)	0 (0)	0 (0)	0 (0)	0 (0)	0 (0)

(B)

In vitro growth (day)	Types of complexes [2]	Number of oocytes used	Number (%) of oocytes at each stage [5]								
			FC	SC	GV	ED	LD	MI	AI-TI	MII	DG
0 [3]	-	16	13 (81)	0 (0)	0 (0)	0 (0)	0 (0)	1 (6)	0 (0)	0 (0)	2 (13)
14	GCs	18	1 (6)	0 (0)	0 (0)	0 (0)	0 (0)	6 (33)	0 (0)	11 (61)	0 (0)
	early MGCs	20	0 (0)	0 (0)	0 (0)	0 (0)	0 (0)	4 (20)	0 (0)	15 (75)	1 (5)
	OCGCs	14	0 (0)	0 (0)	0 (0)	0 (0)	0 (0)	3 (21)	0 (0)	10 (71)	1 (7)
In vivo [4]	-	20	0 (0)	0 (0)	0 (0)	0 (0)	0 (0)	0 (0)	0 (0)	20 (100)	0 (0)

[1] Reconstructed complexes and OCGCs were subjected to *in vitro* growth culture. [2] Reconstructed complexes and OCGCs were subjected to *in vitro* maturation culture after *in vitro* growth culture. DOs were cocultured with GCs and early MGCs. [3] Oocytes were collected from the early antral follicles for culture. [4] Fully grown oocytes were collected from late antral follicles (4–6 mm). [5] FC, filamentous chromatin; SC, stringy chromatin; GV, germinal vesicle I–IV; ED, early diakinesis; LD, late diakinesis; MI, metaphase I; AI-TI, anaphase I and telophase I; MII, metaphase II; DG, degeneration.

In addition, comparison of the datasets of the early group to those of the late CCs group showed that a substantial number of DEGs was detected (up-regulated genes: n = 3,833; down-regulated genes: n = 4,143) (Supplementary Table 2). Genes involved in "organelle organization," "organonitrogen compound metabolic process," and "cellular respiration" were mainly up-regulated in the early group (Fig. 5C). In contrast, genes involved in "protein modification process" were mainly down-regulated in the early group (Fig. 5D). In the comparison of the early and late MGCs groups, *NKD1* (NKD inhibitor of WNT signaling pathway 1) was significantly up-regulated (Supplementary Fig. 2). This gene was notably up-regulated when the early and late CCs groups were compared (Supplementary Fig. 3).

Discussion

After coculture, GCs and early MGCs adhered to DOs, and the complexes were reconstructed. On day 6, regenerated TZPs were observed in oocytes cultured with GCs and early MGCs. In contrast, late MGCs barely adhered to DOs and aggregated tightly, whereas regenerated TZPs were barely observed in the complexes. These results suggest that late MGCs have no ability to elongate TZPs. Because it was difficult to separate late MGCs from aggregated complexes by pipetting, in contrast to GCs and early MGCs, the characteristics of late MGCs appeared to differ from those of GCs and early MGCs. Considering that oocyte-derived factors induce the CC phenotype [3, 16], late MGCs located far from the oocyte may not be as affected by oocyte-derived factors as early MGCs. Another possibility is that the extracellular matrix (ECM) influences GC, CC, and MGC phenotypes [37, 38]. When late MGCs were collected from late antral follicles, they formed more rigid sheet-like structures than early MGCs. ECM components change during follicle development [38], which are able to change the MGC phenotype. Late MGCs collected from late antral follicles may have been in the recruitment or selection phase of the follicular wave and involved in the degeneration process [39].

When growth culture was continued until day 14, DO+GCs and DO+early MGCs developed similarly to OCGCs, although the integrity of DO+GCs and DO+early MGCs during growth culture was lower than that of OCGCs. Although antrum formation in DO+GCs and DO+early MGCs occurred later than in OCGCs, they also formed antrum-like structures. Alam *et al*. [40] proposed that GDF9 and BMP15 produced by bovine oocytes are involved in the formation of antrum-like structures. Therefore, DOs in the reconstructed complexes may communicate with GCs and early MGCs to promote the formation of antrum-like structures in a manner similar to that of OCGCs. Notably, GCs collected from pre-antral follicles also formed antrum-like structures. In mice, oocytes collected from secondary follicles accelerate the differentiation of GCs into primordial follicles and the rate of follicle development [41]. In the present study, GCs may have been promoted to differentiate into CCs and MGCs by oocytes collected from early antral follicles.

After culture, the mean number of TZPs in the DO+GCs and DO+early MGCs increased until reaching numbers similar to those in OCGCs. TZPs likely develop simultaneously with these complexes. Although the mean numbers of TZPs in DO+GCs and DO+early MGCs were significantly lower than those in fully grown oocytes *in vivo*, the mean diameters of oocytes in DO+GCs and DO+early MGCs reached more than 115 µm. Furthermore, more than half of oocytes in DO+GCs and DO+early MGCs adequately progressed to GV stage and matured to MII after maturation culture. The percentage of oocytes was lower in the DO+GC group. Because GCs and DOs were collected from follicles of different sizes, bidirectional communication between these cells may not function well in some complexes. However, considering that CCs provide nutrients for oocyte growth and regulate cGMP levels for meiotic arrest through TZPs [6, 42], TZPs regenerated by GCs and early MGCs are able to support oocyte growth. These results suggest that GCs became CC-like cells, similar to early MGCs, and that the regenerated TZPs

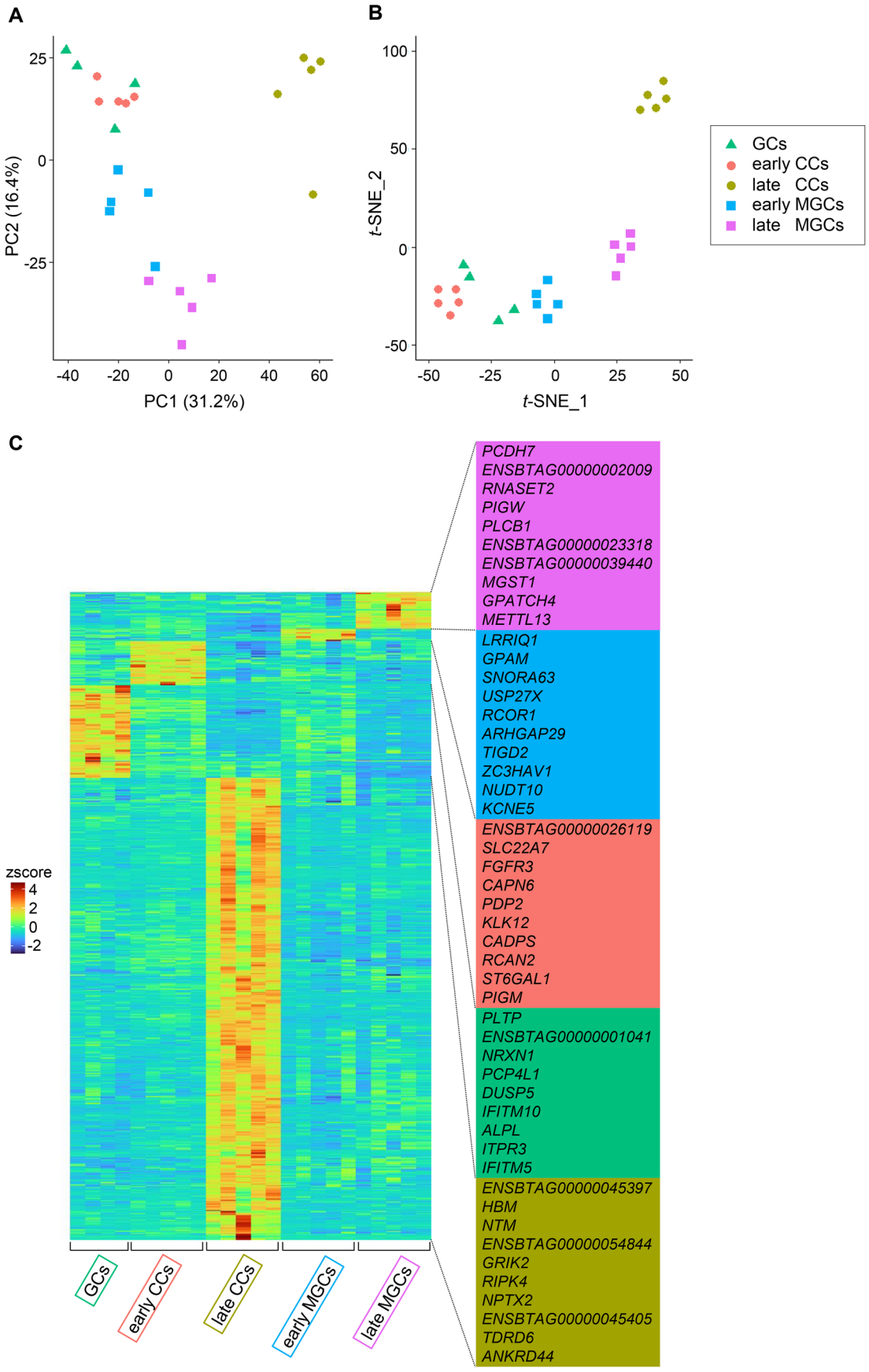

Fig. 4. PCA plot (A), *t*-SNE plot (B), and heatmap visualizing marker gene expression (C) using the datasets from bovine GCs, early CCs, late CCs, early MGCs, and late MGCs. Four GCs collected from secondary follicles, and five CCs and five MGCs each collected from early and late antral follicles were analyzed. (C) Top 10 marker genes for each cell type are shown on the right.

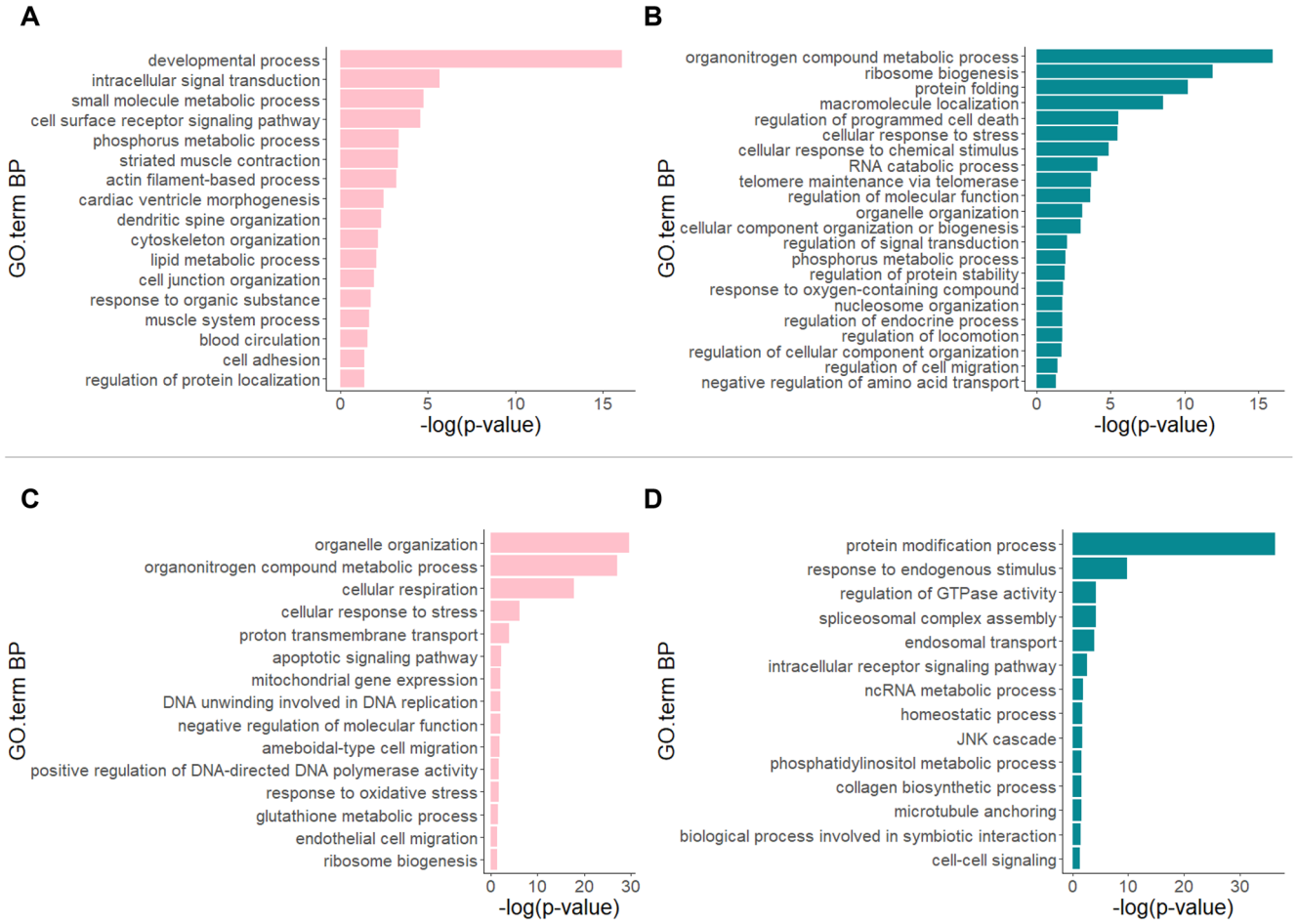

Fig. 5. Representative GO terms (Biological Process, BP) between the group of GCs, early CCs, and early MGCs (referred to as the "early group") and late MGCs group (up-regulated (A) and down-regulated (B)), and between the early group and late CCs group (up-regulated (C) and down-regulated (D)). Comparison of the datasets of the early group to those of the late MGCs group revealed up-regulated genes (FDR < 0.05; $\log_2$ fold change > 0, n = 1,943) and down-regulated genes (FDR < 0.05; $\log_2$ fold change < 0, n = 1,716). Comparison of the datasets of the early group to those of the late CCs group revealed up-regulated genes (FDR < 0.05; $\log_2$ fold change > 0, n = 3,833) and down-regulated genes (FDR < 0.05; $\log_2$ fold change < 0, n = 4,143).

were functional.

Transcriptome analyses indicated that GCs change in two directions to CCs and MGCs at the transcriptome level and that both CCs and MGCs change their transcriptomes during follicle development from the early to late antral stage. The transcriptome changes in MGCs may alter the ability of early and late MGCs to elongate TZPs. In addition, we identified new marker gene candidates for each somatic cell type at different follicular stages. The top 10 marker genes, as well as some DEGs, such as *NKD1*, show potential as marker genes for identifying somatic cells that are able to elongate TZPs and support oocyte growth. *NKD1* inhibits WNT-β-catenin signaling, and activation of WNT signaling is detrimental to folliculogenesis after primary follicle formation [43, 44]. Therefore, *NKD1* may play a role in supporting proper follicular development and oocyte growth. Our data may facilitate a more detailed classification of somatic cells within follicles in further studies.

We compared the datasets of the early group to those of the late MGCs or late CCs groups. The results of GO analysis of the DEGs also indicated a change in transcriptomes. In the early group, "developmental process" was mainly up-regulated compared to in the late MGCs group. Because this GO term refers to the progression of cells from an initial condition to a later condition, the results suggest that GCs, early CCs, and early MGCs differentiated into late MGCs. Interestingly, "actin filament-based process", "dendritic spine organization", and "cytoskeleton organization" were also up-regulated in the early group. Although there is no direct evidence, these genes may be related to the ability of cells to elongate TZPs. "Organelle organization", "organonitrogen compound metabolic process", and "cellular respiration" were mainly up-regulated in the early group compared to the late CCs group. These GO terms refer to the assembly or disassembly of organelles or metabolic processes within a cell. These results also show that GCs, early CCs, and early MGCs changed their intracellular conditions. In contrast, the main genes down-regulated in the early group compared to in the late MGCs and CCs groups were involved in organonitrogen compound or protein synthesis. Additionally, because "regulation of signal transduction," "regulation of endocrine process," "endosomal transport," and "cell-cell signaling" were down-regulated in the early group, MGCs and CCs appeared to acquire functions related to endocrine processes or cell signaling during follicle development.

In conclusion, our results showed that GCs are able to reconstruct complexes with DOs and regenerate TZPs, similar to early MGCs. Furthermore, oocytes in the integrally reconstructed complexes grew fully and acquired meiotic competence, suggesting that the

regenerated TZPs were functional and that GCs and early MGCs became CC-like cells. In contrast, late MGCs lost their ability to elongate TZPs and support oocyte growth. The lost ability to elongate TZPs coincided with transcriptome changes in two directions: from GCs to CCs or MGCs.

Conflict of interests: The authors declare no conflicts of interest associated with this study.

Acknowledgments

We are grateful to the personnel of Kobe-Branch, Animal Biotechnology Center, Livestock Improvement Association of Japan, for providing bovine ovaries. This work was supported in part by a JSPS KAKENHI Grant-in-Aid for Scientific Research (C) Number JP17K08137 awarded to T. Miyano and a JSPS KAKENHI Grant-in-Aid for JSPS Fellows Number JP22KJ2263 awarded to M. Fushii. We acknowledge the help and cooperation of Dr. Tomoya S Kitajima and Dr. Tappei Mishina, Laboratory for Chromosome Segregation, RIKEN Center for Biosystems Dynamics Research, for allowing us to use laboratory equipment and for providing technical assistance.

References

1. **Matzuk MM, Burns KH, Viveiros MM, Eppig JJ.** Intercellular communication in the mammalian ovary: oocytes carry the conversation. *Science* 2002; **296**: 2178–2180. [Medline] [CrossRef]
2. **Hummitzsch K, Anderson RA, Wilhelm D, Wu J, Telfer EE, Russell DL, Robertson SA, Rodgers RJ.** Stem cells, progenitor cells, and lineage decisions in the ovary. *Endocr Rev* 2015; **36**: 65–91. [Medline] [CrossRef]
3. **Juengel JL, McNatty KP.** The role of proteins of the transforming growth factor-β superfamily in the intraovarian regulation of follicular development. *Hum Reprod Update* 2005; **11**: 143–160. [Medline] [CrossRef]
4. **Zhang M, Su YQ, Sugiura K, Xia G, Eppig JJ.** Granulosa cell ligand NPPC and its receptor NPR2 maintain meiotic arrest in mouse oocytes. *Science* 2010; **330**: 366–369. [Medline] [CrossRef]
5. **Conti M, Hsieh M, Zamah AM, Oh JS.** Novel signaling mechanisms in the ovary during oocyte maturation and ovulation. *Mol Cell Endocrinol* 2012; **356**: 65–73. [Medline] [CrossRef]
6. **Clarke HJ.** Regulation of germ cell development by intercellular signaling in the mammalian ovarian follicle. *Wiley Interdiscip Rev Dev Biol* 2018*a*; **7**: 1–22. [Medline] [CrossRef]
7. **Richard S, Baltz JM.** Prophase I arrest of mouse oocytes mediated by natriuretic peptide precursor C requires GJA1 (connexin-43) and GJA4 (connexin-37) gap junctions in the antral follicle and cumulus-oocyte complex. *Biol Reprod* 2014; **90**: 137. [Medline] [CrossRef]
8. **Fair T, Hyttel P, Greve T.** Bovine oocyte diameter in relation to maturational competence and transcriptional activity. *Mol Reprod Dev* 1995; **42**: 437–442. [Medline] [CrossRef]
9. **Hyttel P, Fair T, Callesen H, Greve T.** Oocyte growth, capacitation and final maturation in cattle. *Theriogenology* 1997; **47**: 23–32. [CrossRef]
10. **Tsuji T, Kiyosu C, Akiyama K, Kunieda T.** CNP/NPR2 signaling maintains oocyte meiotic arrest in early antral follicles and is suppressed by EGFR-mediated signaling in preovulatory follicles. *Mol Reprod Dev* 2012; **79**: 795–802. [Medline] [CrossRef]
11. **Russell DL, Robker RL.** Molecular mechanisms of ovulation: co-ordination through the cumulus complex. *Hum Reprod Update* 2007; **13**: 289–312. [Medline] [CrossRef]
12. **Jaffe LA, Egbert JR.** Regulation of mammalian oocyte meiosis by intercellular communication within the ovarian follicle. *Annu Rev Physiol* 2017; **79**: 237–260. [Medline] [CrossRef]
13. **Alam MH, Miyano T.** Interaction between growing oocytes and granulosa cells *in vitro*. *Reprod Med Biol* 2019; **19**: 13–23. [Medline] [CrossRef]
14. **Das D, Arur S.** Regulation of oocyte maturation: Role of conserved ERK signaling. *Mol Reprod Dev* 2022; **89**: 353–374. [Medline] [CrossRef]
15. **Eppig JJ, Wigglesworth K, Pendola F, Hirao Y.** Murine oocytes suppress expression of luteinizing hormone receptor messenger ribonucleic acid by granulosa cells. *Biol Reprod* 1997; **56**: 976–984. [Medline] [CrossRef]
16. **Eppig JJ.** Oocyte control of ovarian follicular development and function in mammals. *Reproduction* 2001; **122**: 829–838. [Medline] [CrossRef]
17. **Diaz FJ, Wigglesworth K, Eppig JJ.** Oocytes are required for the preantral granulosa cell to cumulus cell transition in mice. *Dev Biol* 2007; **305**: 300–311. [Medline] [CrossRef]
18. **Wigglesworth K, Lee KB, Emori C, Sugiura K, Eppig JJ.** Transcriptomic diversification of developing cumulus and mural granulosa cells in mouse ovarian follicles. *Biol Reprod* 2015; **92**: 23. [Medline] [CrossRef]
19. **Sugiura K, Pendola FL, Eppig JJ.** Oocyte control of metabolic cooperativity between oocytes and companion granulosa cells: energy metabolism. *Dev Biol* 2005; **279**: 20–30. [Medline] [CrossRef]
20. **Emori C, Ito H, Fujii W, Naito K, Sugiura K.** Oocytes suppress FOXL2 expression in cumulus cells in mice. *Biol Reprod* 2020; **103**: 85–93. [Medline] [CrossRef]
21. **Fushii M, Yamada R, Lee J, Miyano T.** Reestablishment of transzonal projections and growth of bovine oocytes *in vitro*. *J Reprod Dev* 2021*b*; **67**: 300–306. [Medline] [CrossRef]
22. **Fushii M, Yamada R, Miyano T.** *In vitro* growth of bovine oocytes in oocyte-cumulus cell complexes and the effect of follicle stimulating hormone on the growth of oocytes. *J Reprod Dev* 2021*a*; **67**: 5–13. [Medline] [CrossRef]
23. **Makita M, Miyano T.** Steroid hormones promote bovine oocyte growth and connection with granulosa cells. *Theriogenology* 2014; **82**: 605–612. [Medline] [CrossRef]
24. **Hirao Y, Itoh T, Shimizu M, Iga K, Aoyagi K, Kobayashi M, Kacchi M, Hoshi H, Takenouchi N.** *In vitro* growth and development of bovine oocyte-granulosa cell complexes on the flat substratum: effects of high polyvinylpyrrolidone concentration in culture medium. *Biol Reprod* 2004; **70**: 83–91. [Medline] [CrossRef]
25. **Hirao Y, Shimizu M, Iga K, Takenouchi N.** Optimization of oxygen concentration for growing bovine oocytes *in vitro*: constant low and high oxygen concentrations compromise the yield of fully grown oocytes. *J Reprod Dev* 2012; **58**: 204–211. [Medline] [CrossRef]
26. **Motlík J, Koefoed-Johnsen HH, Fulka J.** Breakdown of the germinal vesicle in bovine oocytes cultivated *in vitro*. *J Exp Zool* 1978; **205**: 377–383. [Medline] [CrossRef]
27. **Hirao Y, Tsuji Y, Miyano T, Okano A, Miyake M, Kato S, Moor RM.** Association between $p34^{cdc2}$ levels and meiotic arrest in pig oocytes during early growth. *Zygote* 1995; **3**: 325–332. [Medline] [CrossRef]
28. **Mishina T, Tabata N, Hayashi T, Yoshimura M, Umeda M, Mori M, Ikawa Y, Hamada H, Nikaido I, Kitajima TS.** Single-oocyte transcriptome analysis reveals aging-associated effects influenced by life stage and calorie restriction. *Aging Cell* 2021; **20**: e13428. [Medline] [CrossRef]
29. **Kim D, Langmead B, Salzberg SL.** HISAT: a fast spliced aligner with low memory requirements. *Nat Methods* 2015; **12**: 357–360. [Medline] [CrossRef]
30. **Chen S, Zhou Y, Chen Y, Gu J.** fastp: an ultra-fast all-in-one FASTQ preprocessor. *Bioinformatics* 2018; **34**: i884–i890. [Medline] [CrossRef]
31. **Li H, Handsaker B, Wysoker A, Fennell T, Ruan J, Homer N, Marth G, Abecasis G, Durbin R. 1000 Genome Project Data Processing Subgroup**. The Sequence Alignment/Map format and SAMtools. *Bioinformatics* 2009; **25**: 2078–2079. [Medline] [CrossRef]
32. **Liao Y, Smyth GK, Shi W.** featureCounts: an efficient general purpose program for assigning sequence reads to genomic features. *Bioinformatics* 2014; **30**: 923–930. [Medline] [CrossRef]
33. **Krijthe JH.** Rtsne: T-distributed stochastic neighbor embedding using a Barnes-Hut implementation. 2015; Available at: https://github.com/jkrijthe/Rtsne.
34. **El Amrani K, Alanis-Lobato G, Mah N, Kurtz A, Andrade-Navarro MA.** Detection of condition-specific marker genes from RNA-seq data with MGFR. *PeerJ* 2019; **7**: e6970. [Medline] [CrossRef]
35. **Robinson MD, McCarthy DJ, Smyth GK.** edgeR: a Bioconductor package for differential expression analysis of digital gene expression data. *Bioinformatics* 2010; **26**: 139–140. [Medline] [CrossRef]
36. **Kolberg L, Raudvere U, Kuzmin I, Adler P, Vilo J, Peterson H.** g:Profiler-interoperable web service for functional enrichment analysis and gene identifier mapping (2023 update). *Nucleic Acids Res* 2023; **51**(W1): W207–W212. [Medline] [CrossRef]
37. **Hwang DH, Kee SH, Kim K, Cheong KS, Yoo YB, Lee BL.** Role of reconstituted basement membrane in human granulosa cell culture. *Endocr J* 2000; **47**: 177–183. [Medline] [CrossRef]
38. **Woodruff TK, Shea LD.** The role of the extracellular matrix in ovarian follicle development. *Reprod Sci* 2007; **14**(Suppl): 6–10. [Medline] [CrossRef]
39. **Ginther OJ, Beg MA, Bergfelt DR, Donadeu FX, Kot K.** Follicle selection in monovular species. *Biol Reprod* 2001; **65**: 638–647. [Medline] [CrossRef]
40. **Alam MH, Lee J, Miyano T.** GDF9 and BMP15 induce development of antrum-like structures by bovine granulosa cells without oocytes. *J Reprod Dev* 2018; **64**: 423–431. [Medline] [CrossRef]
41. **Eppig JJ, Wigglesworth K, Pendola FL.** The mammalian oocyte orchestrates the rate of ovarian follicular development. *Proc Natl Acad Sci USA* 2002; **99**: 2890–2894. [Medline] [CrossRef]
42. **Clarke HJ.** History, origin, and function of transzonal projections: the bridges of communication between the oocyte and its environment. *Anim Reprod* 2018*b*; **15**: 215–223. [Medline] [CrossRef]
43. **Habara O, Logan CY, Kanai-Azuma M, Nusse R, Takase HM.** WNT signaling in pregranulosa cells is required for ovarian folliculogenesis and female fertility. *Development* 2021; **148**: dev198846. [Medline] [CrossRef]
44. **Li L, Ji SY, Yang JL, Li XX, Zhang J, Zhang Y, Hu ZY, Liu YX.** Wnt/β-catenin signaling regulates follicular development by modulating the expression of Foxo3a signaling components. *Mol Cell Endocrinol* 2014; **382**: 915–925. [Medline] [CrossRef]